

# Electron density diagnostic potential of Ar XIV soft X-ray emission lines

G. Y. Liang<sup>a</sup>, G. Zhao<sup>a</sup>, J. L. Zeng<sup>a,b</sup>, J. R. Shi<sup>a</sup>

<sup>a</sup>National Astronomical Observatories, Chinese Academy of Sciences, Beijing  
100012, P. R. China

<sup>b</sup>Department of Applied Physics, National University of Defense Technology,  
Changsha 410073, P. R. China

---

## Abstract

Theoretical electron density-sensitive line ratios  $R_1$ – $R_6$  of Ar XIV soft X-ray emission lines are presented. We found that these line ratios are sensitive to electron density  $n_e$ , and the ratio  $R_1$  is insensitive to electron temperature  $T_e$ . Recent work has shown that accurate atomic data, such as electron impact excitation rates, is very important for reliable determination of the electron density of laboratory and astrophysical plasmas. Present work indicates that the maximum discrepancy of line ratios introduced from different atomic data calculated with distorted wave and R-matrix approximations, is up to 18% in the range of  $n_e = 10^{9-13} \text{ cm}^{-3}$ . By comparison of these line ratios with experiment results carried out in electron beam ion trap (EBIT-II), electron density of the laboratory plasma is diagnosed, and a consistent result is obtained from  $R_1$ ,  $R_2$  and  $R_3$ . Our result is in agreement with that diagnosed by Chen et al using triplet of N VI. A relative higher diagnosed electron density from  $R_2$  is due to its weak sensitivity to electron temperature. A better consistency at lower  $T_e$  indicates that temperature of the laboratory plasma is lower than  $\log T_e (\text{K}) = 6.5$ . Comparison between the measured and theoretical ratios

reveals that 32.014 Å line is weakly blended by lines from other Ar ions, while 30.344 Å line is strongly contaminated.

Key words: Soft X-ray; Electron density; Line intensity ratio; Diagnostic

---

## 1 Introduction

Spectroscopy has exhibited its great importance for diagnostic of laboratory and astrophysical plasmas. Emission lines arising from  $n = 2 \rightarrow n = 1$  transitions of B-, C- and N-like ions have been frequently observed in solar extreme-ultraviolet spectra [1]. They have been extensively used to determine electron temperature and/or density of stellar coronae through line intensity ratios. Keenan et al. [2-4] presented electron density-sensitive ratios for B-like ions including Si X, Ar XIV and Ca XVI etc. For C-like ions including S XI, Ca XV, Fe XXI and Ar XIII, the electron density-sensitive ratios were also given by Keenan et al. [5-8]. For N-like ions, to our best knowledge, the electron density-sensitive ratios were presented only for S X [9]. Using the ratios from these ions' lines, accurate electron densities have been obtained, which are consistent with those from iron ions with same temperatures of maximum fractional abundance in ionization equilibrium [10]. Another benefit using these line ratios is that the uncertainty due to ionization equilibrium and element abundance has been eliminated.

With the launch of a new generation of X-ray satellites, including Chandra and XMM, a large amount of high quality spectra with high spectral resolution

---

Corresponding author: Gui-Yun Liang

Email address: gyliang@bao.ac.cn (G.Y.Liang).

and high effective area have been obtained for nearly all classes of astrophysical X-ray sources [11-17]. This will allow us to estimate physical parameters such as the electron temperature and density of the stellar X-ray corona. The temperature has long been available before the launch of the two satellites, while the density determination of X-ray emitting layer becomes possible until the launch of satellites with the high-spectral resolution. Spatial information of stars could be assessed indirectly from relationship between electron density and emission measure ( $EM = n_e^2 V$ ). For reliable determination of the electron density and temperature, accurate atomic data is very important, especially electron impact excitation rates and oscillator strengths [8].

Currently, the electron density is mainly determined using triplet line ratios (resonance, inter-combination and forbidden lines) of H e-like ions for line formation regions. Ness et al. [18] and Testa et al. [19] present an extensive investigation using those H e-like ions for stars with different activity levels, and disclose that the electron density of stellar coronae does not exceed  $5 \times 10^{12} \text{ cm}^{-3}$ . One reason of the extensive application of H e-like ions is that a larger amount of reliable atomic data is available, because the atomic data calculation of K-shell ions is relatively simple. And some laboratory experiments conducted in Tokamak, electron beam ion traps (EBIT) and intense laser-matter interaction have been carried to benchmark the theoretical calculation for K-shell ions [20,21]. Many L-shell emission lines of iron ions have been detected for star coronae. The temperature structure of the X-ray emitting layers have been obtained using these iron lines. However, further investigation is still necessary to depict out the structure of the stellar coronae and to explain heating mechanism.

In X-ray spectra of stars with various activity, the L-shell emission lines of non-

iron elements including Si, S, Ar and Ca have also been detected. But recent studies revealed that there are large uncertainties for the atomic data of these ions. Fortunately, a large project | Emission Line Project supported by the Chandra X-ray Observatory, has been opened to complete a comprehensive catalog of astrophysically relevant emission lines in support of new-generation X-ray observatories. Lepson et al. [22] recently made an experiment for highly charged Ar ions in EB II-II to benchmark theoretical calculation. The intensity ratios of the L-shell emission lines of these non-iron ions might be used for direct density estimations of stellar coronae and fusion plasma. Therefore the exploration and calibration of the line intensity ratios of the L-shell emission lines of the non-iron elements, such as Si, S, Ar and Ca, are necessary in the next few years.

Argon is an abundant element, and has been detected in solar and solar-like stars, such as Capella [13], Algol [23] and AU Mic [24]. For example, the emission lines arising from  $n = 3 \rightarrow 2$  transitions of Ar XV I have been identified by Audard et al. [13], and  $3d \rightarrow 2p$  transition lines located near 27.043 Å of Ar XV have also been identified in our previous work [25]. In ionization equilibrium condition [10], the temperature of maximum Ar XIV fractional abundance has a same value with that of He-like Ne. However the triplets of He-like Ne are strongly blended by forest-like features of highly charged Fe ions [26]. So the features of Ar XIV may give the density information in Ne IX ion formation region. At present, APEC database is the most complete and has been extensively used in X-ray spectral analyses for stars. In fact APEC extends Chianti database by including some experimental values of highly charged iron ions. In Chianti database, emission lines of Ar XIV are also included. However all the collision rates are results with distorted wave (DW)

approximation and using less configurations. Therefore the exploration of the density-sensitive line ratios of highly charged Ar XIV using more accurate atomic data will be meaningful.

In this paper we present calculations of electron density-sensitive line intensity ratios of Ar XIV in X-ray line formation region. Present calculation of atomic structure includes more configurations than previous work, and some excitation rates are replaced by data from R-matrix method. By comparing these ratios with experimental ones conducted by Lepson et al. [22] in the Lawrence Livermore electron beam ion traps EBIT-II, the electron density of the laboratory plasma is determined.

## 2 Theoretical line ratios

The model ion for Ar XIV consists of 152 one-structure energy levels belonging to the configurations  $2s^22p$ ,  $2s2p^2$ ,  $2p^3$ ,  $2s^23l$ ,  $2s2p3l$ ,  $2p^23l$  ( $l = s;p;d$ ),  $2s^2n1$  ( $n = 4;5;6$  and  $l = n - 1$ ).

Electron impact excitation rates are obtained by performing numerical integration of collision strengths over a Maxwellian distribution. The collision strengths among the lowest 152 energy levels, along with the spontaneous radiative decay rates and energy levels were calculated using the Flexible Atomic Code (FAC) developed by Gu [27,28]. The atomic structure calculation in FAC is based on the fully relativistic configuration interaction approximation, while the electron impact collision strengths are calculated in the relativistic DW approximation. These data are available electronically from the authors (gyliang@bao.ac.cn) on request. For the electron impact excitation rates

among the lowest 15 levels, we adopted recent results of Keenan et al. [8], in which a more accurate method | R-matrix (Burke and Robb [29]) is adopted. As noted by, for example, Seaton [30], excitation by protons will be important for the lowest levels. This will affect the X-ray emission lines indirectly. In the present analysis we have employed the rates of Foster, Keenan & Reid [31], which were calculated using a close-coupled impact-parameter method.

Using the atomic data discussed above in conjunction with rate equations, relative Ar XIV level populations were derived for a range of electron temperatures and densities. The rate equations are given as [25,32,33]

$$N_j \left[ \sum_{i < j} A_{ji} + n_e \left( \sum_{i < j} C_{ji}^d + \sum_{i > j} C_{ji}^e \right) \right] = \sum_{i > j} N_i A_{ij} + n_e \left( \sum_{i < j} N_i C_{ij}^e + \sum_{i > j} N_i C_{ij}^d \right);$$

where the superscript e and d refer to electron excitation and deexcitation,  $N_j$  is the number density of level j, and  $n_e$  is the electron density. In the calculations, following assumptions were made: (i) photon-excitation and deexcitation rates are negligible in comparison with the corresponding collision rates; (ii) ionization to and recombination from other ionic levels are slow compared with bound-bound rates; (iii) the plasma is optically thin. Generally, the line intensity for a given transition line  $j_i$  is given by

$$I_{ji} = N_j A_{ji};$$

In order to correctly understand the astrophysical spectra, Lepson et al. [22] carried out an experiment in Lawrence Livermore electron beam ion traps EB II-II for Ar at three different energies of 600, 650 and 1000 eV. This is part of a large project to complete a comprehensive catalog of astrophysically relevant emission lines in support of new-generation X-ray observatories. In this experiment, several emission lines of Ar XIV were detected, as shown in

Table 1

Experimental wavelength [22] and line identification of Ar XIV. The theoretical intensity ratios are calculated at a temperature ( $\log T_e$  (K) = 6.5) and density ( $5.6 \cdot 10^{10} \text{ cm}^{-3}$ ). The intensities are normalized to that of 27.469 Å line.

Wavelength (Å)		Relative intensity		Transition			
Exp:	HULLAC	FAC	Measured	HULLAC	FAC		
27:469	27:517	27:470	1:00	1:00	1:00	$2s^2 3d_{3=2}$	$2s^2 2p_{1=2}$
27:631	27:674	27:629	0:95	1:25	0:76	$2s^2 3d_{5=2}$	$2s^2 2p_{3=2}$
...	27:688	27:642 <sup>b</sup>	...	0:19	0:20	$2s^2 3d_{3=2}$	$2s^2 2p_{3=2}$
28:223	28:332	28:329	0:20	0:25	0:25	$((2s2p_{1=2})_1 3d_{5=2})_{5=2}$	$((2s2p_{1=2})_1 2p_{3=2})_{3=2}$
30:215	30:342	30:236	0:20	0:25	0:20	$((2s2p_{3=2})_2 3s)_{3=2}$	$((2s2p_{1=2})_1 2p_{3=2})_{5=2}$
30:344	30:476	30:367	0:15	0:25	0:41	$((2s2p_{1=2})_1 3s)_{1=2}$	$((2s2p_{1=2})_1 2p_{3=2})_{3=2}$
		31:360				$((2s2p_{1=2})_1 3s)_{1=2}$	$2s(2p^2)_0$
32:014	32:161	32:071	0:30	0:19	0:21	$2s^2 3p_{3=2}$	$((2s2p_{1=2})_1 2p_{3=2})_{5=2}$
...	32:215	32:125 <sup>b</sup>	...	0:13	0:24	$2s^2 3p_{1=2}$	$((2s2p_{1=2})_1 2p_{3=2})_{3=2}$

<sup>b</sup> denotes a blended line

Table 1. Theoretical predictions of line intensities, including HULLAC [22] and FAC calculations by us, are also presented.

By resolving rate equations, we found that the following emission line intensity ratios of Ar XIV ion, are sensitive to electron density:

$$R_1 = I(27:631 \text{ Å})/I(27:469 \text{ Å});$$

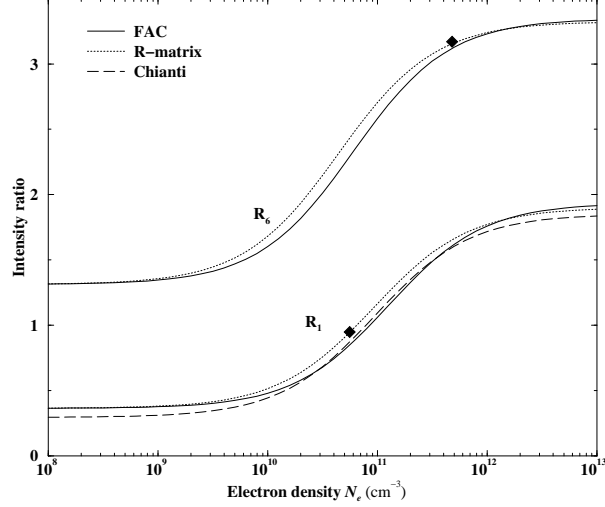


Fig. 1. The theoretical Ar XIV emission line ratios  $R_1$  and  $R_6$ , plotted as a function of electron density ( $n_e$  in  $\text{cm}^{-3}$ ) at the temperature of maximum Ar XIV fractional abundance in ionization equilibrium,  $\log T_e$  (K) = 6.5. Filled diamonds and Dashed curve are experimental values measured in EB IT-II by Lepson et al. [22], and Chianti prediction, respectively.

$$R_2 = I(27:631 \text{ \AA})/I(28:223 \text{ \AA});$$

$$R_3 = I(27:631 \text{ \AA})/I(30:215 \text{ \AA});$$

$$R_4 = I(27:631 \text{ \AA})/I(30:344 \text{ \AA});$$

$$R_5 = I(27:631 \text{ \AA})/I(31:360 \text{ \AA});$$

$$R_6 = I(27:631 \text{ \AA})/I(32:014 \text{ \AA});$$

Therefore they may be useful for the electron density diagnostics for all kinds of hot plasma with sufficient signal-to-noise ratio. Figures 1 | 4 show the theoretical line intensity ratios as a function of the electron density at temperature ( $\log T_e$  (K) = 6.5) of maximum Ar XIV fractional abundance in ionization equilibrium [10]. Predictions of ratios  $R_3$  and  $R_5$  are much larger than one, so the determination of electron density will be very difficult due to extremely faint lines involved. In these figures, the solid lines refer to results using the excitation rates obtained from DW approximation, while the dotted lines refer to results using the excitation rates for the lowest 15 energy levels obtained from R-matrix approximation [8]. The discrepancies between DW and

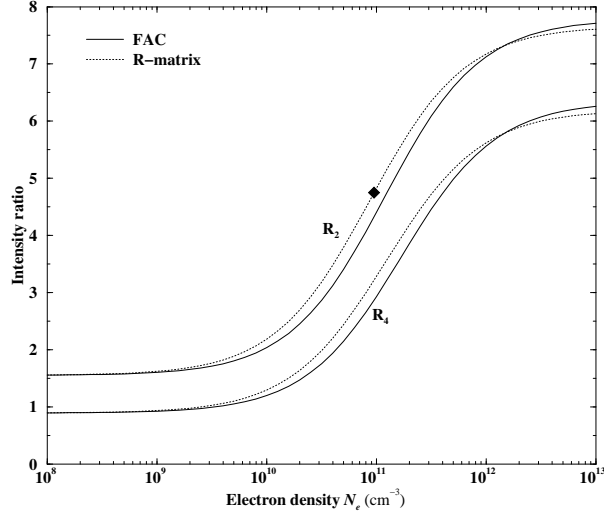


Fig. 2. The theoretical Ar XIV emission line ratios  $R_2$  and  $R_4$ , plotted as a function of electron density ( $n_e$  in  $\text{cm}^{-3}$ ) at the temperature of maximum Ar XIV fractional abundance in ionization equilibrium,  $\log T_e$  (K) = 6.5. Filled diamond are experimental values measured in EBIT-II by Lepson et al. [22].

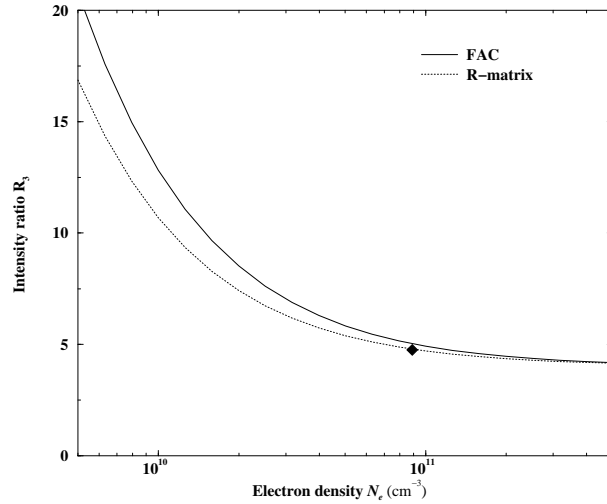


Fig. 3. The theoretical Ar XIV emission line ratios  $R_3$ , plotted as a function of electron density ( $n_e$  in  $\text{cm}^{-3}$ ) at the temperature of maximum Ar XIV fractional abundance in ionization equilibrium,  $\log T_e$  (K) = 6.5. Filled diamond are experimental values measured in EBIT-II by Lepson et al. [22].

R-matrix calculation reach up to 15% at  $n_e = 10^{12} \text{ cm}^{-3}$ , which indicates that the resonance excitation effect is important in the calculation of the electron impact excitation rates. Chianti prediction exhibits a similar result with the

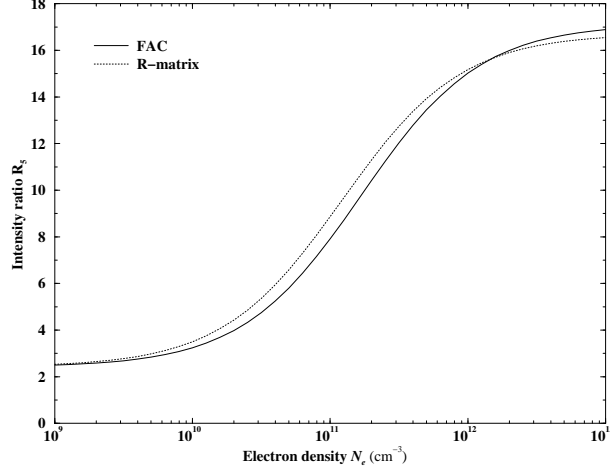


Fig. 4. The theoretical Ar XIV emission line ratios  $R_5$ , plotted as a function of electron density ( $n_e$  in  $\text{cm}^{-3}$ ) at the temperature of maximum Ar XIV fractional abundance in ionization equilibrium,  $\log T_e$  (K) = 6.5.

FAC prediction in density-sensitive region as shown in Fig. 1. For clarity, CHIANTI prediction is shown only for ratio  $R_1$ . APEC shows similar result with CHIANTI prediction due to same data adopted for Ar XIV. An inspection of the figures also tells us that the ratios are sensitive to the electron density. For example  $R_1$  and  $R_2$ , vary by factors of 4.4 and 4.3 respectively, at  $n_e = 10^9$  and  $10^{12} \text{ cm}^{-3}$ . Moreover the ratio  $R_1$  is insensitive to electron temperature. For example, a change in  $T_e$  of 0.2 dex (i.e. 58%) leads to a less than 1% variation at  $n_e = 10^9 \text{ cm}^{-3}$ , up to 3% at  $n_e = 10^{11} \text{ cm}^{-3}$ , as shown in Fig. 5. The sensitivity of the line intensity ratio  $R_1$  to electron density, combined with its insensitivity to  $T_e$ , makes it very useful for the density diagnostics for laboratory and astrophysical plasmas.

### 3 Results and discussion

Applying present line intensity ratios, we diagnose the electron density of Ar laboratory plasma conducted by Lepson et al. [22] in EBIT-II. In the

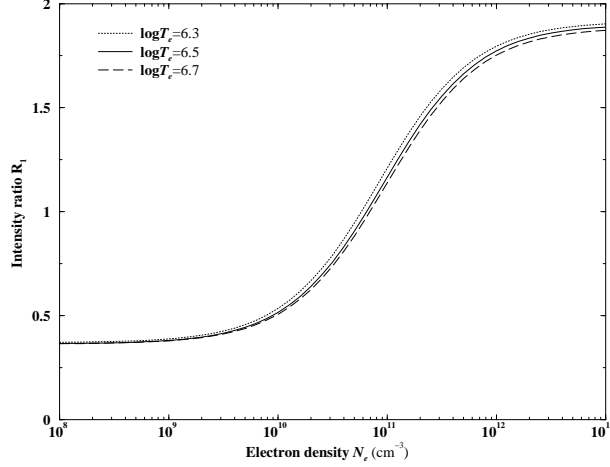


Fig. 5. The theoretical Ar X IV emission line ratio  $R_1$ , plotted as a function of electron density ( $n_e$  in  $\text{cm}^{-3}$ ) at temperature  $\log T_e$  (K) = 6.3 (dotted line), 6.5 (solid line) and 6.7 (dashed line)

experiment, energy of electron beam is fixed at 1.0 KeV. However, the energy will become lower than 1.0 KeV when the electrons interact with cold Ar gas in trap region. The temperature of produced Ar plasma is not given by Lepson et al. [22]. For detailed information of the experiment, you can refer the paper written by Lepson et al. [22]. Recently, Chen et al. [34] measured the electron density ( $6.0 \times 10^{10} \text{cm}^{-3}$ ) of the laboratory plasma using triplet line intensity ratio of He-like N ion.

In Table 1, we present the measured intensities relative to that of the line at 27.469 Å, along with the theoretical results including the HULLAC [22] and FAC calculations by us. In the theoretical calculation, the electron temperature adopted here is  $\log T_e$  (K) = 6.5 which corresponds to maximum Ar X IV fractional abundance in ionization equilibrium [10], while the electron density is  $n_e = 5.6 \times 10^{10} \text{cm}^{-3}$ . In the ionization equilibrium condition, the fraction of Ar X IV as a function of temperature has a steep peak at  $\log T_e$  (K) = 6.5. Since emissivity almost comes from plasma with this temperature, we assume the produced plasma is isothermal plasma with temperature  $\log T_e$  (K) = 6.5. Table

1 shows that our results are in agreement with experimental measurements and are better than the HULLAC calculation in wavelength. For the relative intensities, our calculation also agree with experimental measurement except for the line at 30.344 Å .

Above section has shown that the ratio  $R_1$  is sensitive to the electron density  $n_e$ , while it is insensitive to the electron temperature  $T_e$ . Obviously this ratio is a good diagnostic tool for the electron density  $n_e$ . Moreover, the laboratory measurement and theoretical calculation indicate that emission lines relevant to the ratio  $R_1$  are the strongest lines of Ar XIV and not contaminated by other Ar lines. So we can use  $R_1$  to diagnose the electron density of the laboratory plasma. By comparison between the measured value and theoretical calculation as shown by the filled diamond in Fig. 1, the electron density  $n_e = 5.6 \times 10^{10} \text{ cm}^{-3}$  is derived. This result is consistent with value  $6.0 \times 10^{10} \text{ cm}^{-3}$  recently diagnosed by Chen et al. [34] using triplet line intensity ratio of He-like N ion.

Table 2 shows the diagnosed electron densities of the EB II-II plasma from different line ratios. They are obtained by comparing the theoretical line ratios with the experimental measurements which are indicated by the filled diamonds in Fig. 1 | 3. Given the uncertainties in the theoretical and measured line ratios, the derived values of  $\log n_e$  would be expected to be accurate within 0.3 dex. The results corresponding to  $\log T_e (\text{K}) = 6.5$  shown in Table 2, indicate that the discrepancies of diagnosed electron density from  $R_1; R_2$  and  $R_3$  do not exceed 0.25 dex. The consistency of the diagnosed electron density from  $R_1; R_2$  and  $R_3$  further confirms that our results are reliable.  $R_2$  predicts a relative higher electron density compared to  $R_1$  and  $R_3$  at  $\log T_e (\text{K}) = 6.5$ . Part of the reason may be due to the temperature sensitivity of  $R_2$  as shown in Fig.

Table 2

The diagnosed electron density of the EB II plasma assuming the isothermal plasma with three different temperatures  $\log T_e$  (K) = 6.3, 6.5 and 6.7.

	Electron density $n_e$ ( $10^{10} \text{ cm}^{-3}$ )					
	$R_1$	$R_2$	$R_3$	$R_4$	$R_5$	$R_6$
$\log T_e = 6.3$	5:1	6:0	7:6		45:5	
$\log T_e = 6.5$	5:6	9:5	9:0		55:7	
$\log T_e = 6.7$	6:1	14:4	10:7		95:8	

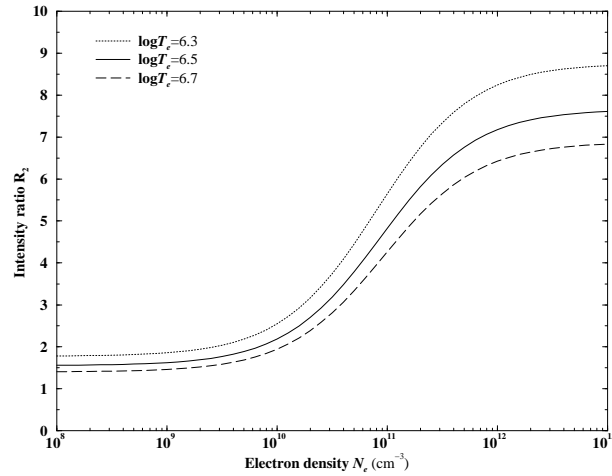


Fig. 6. The theoretical Ar XIV emission line ratio  $R_2$ , plotted as a function of electron density ( $n_e$  in  $\text{cm}^{-3}$ ) at temperature  $\log T_e$  (K) = 6.3 (dotted line), 6.5 (solid line) and 6.7 (dashed line)

6. A change in  $T_e$  of 0.2 dex leads to 10% variation in  $R_2$  at  $n_e = 10^{11} \text{ cm}^{-3}$ , which can explain the relative higher diagnosed electron density from it. The measured value of  $R_4$  (6.33) exceeds the high density-sensitive limit, so no electron density can be derived as shown by Fig. 2. The line at 31.360 Å is strongly shadowed by Ar X II line at 31.374 Å [22], therefore no reliable measured line intensity is available, which results in large uncertainty in  $R_5$ . The

line at 32.014 Å blends with weak lines of Ar X III at this wavelength, so a higher electron density is derived from  $R_6$ .

Fig. 6 shows that the ratio  $R_2$  is slightly sensitive to the electron temperature. At a lower electron temperature  $\log T_e$  (K) = 6.3, the derived electron density from  $R_2$  can be consistent with that from  $R_1$  and  $R_3$  within a much smaller uncertainty range (25%). Decreasing temperature from  $\log T_e$  (K) = 6.5 to 6.3, the uncertainty range decreases from 78% to 25% as shown in Table 2. Which indicates that the electron temperature of the laboratory plasma is lower than that of maximum Ar X IV fractional abundance in ionization equilibrium.

Table 3 lists the experimental and theoretical intensity ratios at  $\log T_e$  (K) = 6.5 and  $n_e = 5.6 \times 10^{10} \text{ cm}^{-3}$ . For ratios  $R_2$  and  $R_6$ , poor consistencies between the measurements and theoretical calculations can be found in Table 3. The temperature-sensitivity can explain the discrepancy for  $R_2$ , while the contribution from those weakly Ar X III lines around 32.014 Å line can explain the deviation for  $R_6$ . The large discrepancy for  $R_4$  may be due to that the 30.344 Å line is strongly contaminated by Ar X III lines located at this wavelength region [22].

#### 4 Conclusion

We found that intensity ratios  $R_1 | R_6$  of emission lines arising from  $n = 3 \rightarrow 2$  transitions of Ar X IV are sensitive to electron density. And the ratio  $R_1$  is insensitive to electron temperature. For example, a change in  $n_e$  of 1 dex leads to variation with factor 4.4 in  $R_1$ , while a change in  $T_e$  of 0.2 dex (i.e. 58%) leads to a less than 1% variation at  $n_e = 10^9 \text{ cm}^{-3}$ , up to 3% at  $n_e = 10^{11}$

Table 3

Experimental and theoretical intensity ratios. The experimental values are from Lepson's work [22]

	Ratio Experiment	Theory
R <sub>1</sub>	0:95	0:96
R <sub>2</sub>	4:75	3:87
R <sub>3</sub>	4:75	4:81
R <sub>4</sub>	6:33	2:35
R <sub>5</sub>		6:13
R <sub>6</sub>	3:17	2:10

$\text{cm}^{-3}$ . Therefore  $R_1$  is very useful for the electron density diagnostics of laboratory and astrophysical plasmas. The two lines of Ar XIV relevant to  $R_1$  are the strongest, and no blended Ar lines have been detected in the experiment conducted by Lepson et al. [22] in EB II-II. By comparison between the experimental value and theoretical line intensity ratio  $R_1$ , an electron density of  $n_e = 5.6 \times 10^{10} \text{cm}^{-3}$  of the laboratory plasma is derived, which is consistent with value  $6.0 \times 10^{10} \text{cm}^{-3}$  recently diagnosed by Chen et al. [34] using triplet line of N VI. The derived electron densities from  $R_2$  and  $R_3$ , are also consistent with that within uncertainty, which further confirms that our results are reliable. In addition, the electron density derived from these ratios eliminates the uncertainty from ionization balance and electron abundance determination. At a lower logarithmic electron temperature ( $\log T_e (\text{K}) = 6.3$ ), the derived electron density from  $R_2$  can be consistent with that from  $R_1$  and  $R_3$  within

a much smaller uncertainty range (25%). Which indicates the temperature of the laboratory plasma is lower than  $\log T_e (K) = 6.5$ .

#### Acknowledgments

This work was supported by the National Natural Science Foundation of China under Grant No. 10373014 and 10403007, and the Chinese Academy of Sciences under Grant No. KJCX2-W 2.

#### References

- [1] Landi E, Feldman U, Dere KP. *Astrophys J Suppl* 2002;139:281
- [2] Keenan FP, Pinfield DJ, Woods VJ, et al. *Astrophys J* 1998;503:953
- [3] Keenan FP, Pinfield DJ, Mathioudakis M, et al. *Solar Physics* 2000;197:253
- [4] Keenan FP, Aggarwal KM, Katsiyannis AC, et al. *Solar Physics* 2003;217:225
- [5] Keenan FP, Conlon ES, Foster VJ, et al. *Solar Physics* 1993;145:291
- [6] Keenan FP, O'Shea E, Thomas RJ, et al. *Mon Not R Astron Soc* 2000;315:450
- [7] Keenan FP, Aggarwal KM, Williams DR, et al. *Mon Not R Astron Soc* 2001;326:1387
- [8] Keenan FP, Katsiyannis AC, Reid RHG, et al. *Mon Not R Astron Soc* 2003;346:58
- [9] Keenan FP, Katsiyannis AC, Widing KG, et al. *Astrophys J* 2004;601:565

- [10] Mazzotta P, Mazzitelli G, Colafrancesco S, Vittorio N. *Astrophys J Suppl* 1998;133:403
- [11] Brinkman AC, Gunsing CJT, Kaastra JS, et al. *Astrophys J* 2000;530:L111
- [12] Canizares CR, Huenemoerder DP, Davis DS, et al. *Astrophys J* 2000;539:L41
- [13] Audard M, Behar E, Gudel M, et al. *Astron & Astronophys* 2001;365:L329
- [20] Brinkman AC, Behar E, Gudel M, et al. *Astron & Astronophys* 2001;365:L324
- [15] Ness J-U, Mewe R, Schmitt JHMM, et al. *Astron & Astronophys* 2001;367:282
- [16] Rasmussen AP, Behar E, Kahn SM, et al. *Astron & Astronophys* 2001;365:L231
- [17] Flanagan KA, Canizares CR, Dewey D, et al. *Astrophys J* 2004;605:230
- [18] Ness J-U, Gudel M, Schmitt JHMM, Audard M, Telleschi A. *Astron & Astronophys* 2004;427:667
- [19] Testa P, Drake JJ, Peres G. *Astrophys J* 2004;617:508
- [20] Beiersdorfer P, Osterheld AL, Phillips TW, et al. *Phys Rev E* 1995;52:1980
- [21] Skobelev IY, Faenov AY, Dyakin VM, et al. *Phys Rev E* 1997;55:3773
- [22] Lepson JK, Beiersdorfer P, Behar E, Kahn SM. *Astrophys J* 2003;590:604
- [23] Ness J-U, Schmitt JHMM, Burwitz V, et al. *Astron & Astronophys* 2002;387:L032
- [24] Magee HRM, Gudel M, Audard M, et al. *Adv Space Res* 2003;32:1149
- [25] Liang GY, Zhao G, Zeng JL and Shi JR. *Mon Not Astron Soc* 2004;350:298

- [26] Ness J-U , Brickhouse NS, Drake JJ, Huenem oerder DP . A strophys J 2003;598:1277
- [27] Gu M F . A strophys J 2003;582:1241
- [28] Gu M F . A strophys J 2003;593:1249
- [29] Burke PG , Roob W D . Adv At M olPhys 1975;11 :143
- [30] Seaton M J. M on Not A stron Soc 1964;127:191
- [31] Foster VJ, Keenan FP, Reid RHG Atom Data Nucl data Tables 1997;67:99
- [32] Behar E , Cottam J, Sahn SM . A strophys J 2001;548:966
- [33] Liang G Y , B ian X , Zhao G . Chinese Physics 2004;13 :891
- [34] Chen H , Beiersdorfer P , Heeter LA , et al. A strophys J 2004;611 :598